

## INTERACTIONS OF RADIATION AND PARTICLES WITH CONDENSED MATTER

PACS numbers: 61.72.uf, 68.35.bj, 81.40.Np, 81.40.Wx, 81.65.-b

### Hydrogen Treatment of Silicon Surface Following Proton Irradiation

A. Vasiljev\*, T. Vasyliev\*, A. Vdovenkov\*, O. Kukharenko\*\*,\*\*,  
T. Doroshenko\*\*\*, and M. Tolmachov\*\*

\**Taras Shevchenko National University of Kyiv,  
Institute of High Technologies,  
60 Volodymyrska Str.,  
UA-01033 Kyiv, Ukraine*

\*\**Cooperation Center ‘Kyiv Scanning Ion Microprobe’  
of Taras Shevchenko National University of Kyiv  
and Company ‘T.M.M.’ Limited,  
50A Mashynobudivna Str.,  
UA-03067 Kyiv, Ukraine*

\*\*\**V. E. Lashkaryov Institute of Semiconductor Physics, N.A.S. of Ukraine,  
Laboratory of Optoelectronic Molecular-Semiconductor Systems,  
41 Nauky Ave.,  
UA-03028 Kyiv, Ukraine*

The present work demonstrates that hydrogen treatment is capable to destroy and to split the surface of silicon single crystal. Hydrogen treatment is performed after the proton irradiation of the silicon surface. All operations with the silicon single crystal are performed at room temperature. The surface of the crystal is irradiated with a proton beam. The proton energy in the beam is 1.5 MeV. The energy spread did not exceed 150 eV. The integral radiation fluence is  $2 \cdot 10^{14}$  p/cm<sup>2</sup>. Such a dose of radiation is sufficient to form a thin layer with a high density of radiation defects at a depth of 30 μm under the surface. The existence of this thin layer is confirmed after chemical manifestation by observations on the electron microscope. After irradiation, an electrolytic saturation of the silicon sample with hydrogen is carried out through

---

Corresponding author: Anatoliy Heorgiyovich Vasiljev  
E-mail: a.g.vasyliev56@gmail.com

Citation: A. Vasiljev, T. Vasyliev, A. Vdovenkov, O. Kukharenko, T. Doroshenko, and M. Tolmachov, Hydrogen Treatment of Silicon Surface Following Proton Irradiation, *Metallofiz. Noveishie Tekhnol.*, **42**, No. 10: 1325–1334 (2020),  
DOI: [10.15407/mfint.42.10.1325](https://doi.org/10.15407/mfint.42.10.1325).

the irradiated surface. During electrolysis, the irradiated surface of the sample uses as a cathode and the graphite electrode—as an anode. The solution of 10%  $H_2SO_4$  and 2% KF in water is used for electrolysis. The electrolytic current density is  $57.15 \text{ mA/cm}^2$ . After 10 minutes of electrolytic saturation of the sample with hydrogen, part of the sample is split. A portion of the irradiated sample is split along the layer with a high density of radiation defects.

**Key words:** proton irradiation, radiation defects, hydrogen treatment, nanoporous silicon surface.

У роботі показано, що воднева обробка здатна руйнувати та відколювати поверхню монокристалічного кремнію. Водневу обробку проводили після опромінення протонами поверхні кремнію. Всі дії з монокристалом кремнію виконували за кімнатної температури. Поверхню кристалу опромінили пучком протонів. Енергія протонів у пучку становила 1,5 МeВ. Розкид енергій не перевищував 150 еВ. Інтегральна доза опромінення протонами склала  $2 \cdot 10^{14}$  протон/ $\text{cm}^2$ . Такої дози опромінення вистачило для утворення на глибині 30 мкм під поверхнею тонкого шару з високою густинною радіаційних дефектів. Наявність такого шару після хімічного проявлення підтверджена спостереженнями на електронному мікроскопі. Після опромінення через опромінену поверхню проведено електролітичне насичення зразка кремнію Гідрогеном. Під час електролізу опромінена поверхня зразка слугувала катодом, а графітовий електрод анодом. Для електролізу використовували розчин 10%  $H_2SO_4$  та 2% KF у воді. Густина електролітичного струму була  $57,15 \text{ mA/cm}^2$ . Після 10 хвилин електролітичного насичення зразка Гідрогеном відбулося сколення зразка. Відкололася частина опроміненого зразка вздовж шару з високою густиною радіаційних дефектів.

**Ключові слова:** опромінення протонами, радіаційні дефекти, воднева обробка, нанопорувата поверхня кремнію.

(Received February 28, 2020; in final version, August 18, 2020)

## 1. INTRODUCTION

The hydrogen-materials systems have unique physical features due to the nature of the hydrogen atom. Hydrogen exposure is a reversible, manageable and exceptionally strong external influence on materials. The reversibility and controllability of the hydrogen effect are due to the high rate of hydrogen penetration into the solid and the extremely high diffusion mobility of hydrogen in the crystal lattice. Therefore, the hydrogen can be introduced into the material quickly, metered and controlled, and after the hydrogen treatment, the hydrogen can be left the material or evacuated from it.

Hydrogen impact on materials is a very strong and fundamental impact. Indeed, the saturation of the material with hydrogen changes its

chemical composition. Accordingly, there is a mismatch of the formed material with the initial external conditions of existence. In other words, saturation with hydrogen, at specially selected conditions, translates the material into a non-equilibrium state. There is a thermodynamic need for phase and structural transformations [1, 2]. Another fundamental factor of hydrogen impact on materials is purely kinetic. Dissolved hydrogen greatly accelerates the diffusion of atoms of the material components [3, 4].

The development of the electronic industry is increasingly linked to the use of thin layers of semiconductor single crystals. Therefore, the development of technologies for producing such layers is very important. Today, Smart Cut technology is used to obtain a thin single crystal layer. The purpose of this technology is to separate the surface layer of the semiconductor wafer. It is based on the creation of an ultra-thin porous layer beneath the surface that arises after irradiation of the surface of the plate with protons. The pores in this layer are filled with hydrogen. The further separation of the silicon layer is due to annealing. It is not possible to separate the surface of the plate with insufficient radiation fluence. To separate the surface layer of the plate the integral fluence of irradiation must be higher than  $10^{17}$  p/cm<sup>2</sup> [5]. Therefore, for the successful implementation of Smart Cut technology, there are strict requirements for proton beams irradiated the surface of a semiconductor crystal. Such requirements make the technology quite expensive to irradiate the surface.

The purpose of this work is to separate the surface layer of silicon after irradiation with protons of a small fluence by means of supplementation of the technology by further electrolytic saturation of the sample with hydrogen. The use of hydrogen treatment of proton-irradiated surfaces can reduce the cost of surface separation technologies. Presently active properties of nanoporous semiconductor surfaces have been studied [6–8]. The controllability of the proton beam by energy and space with subsequent hydrogen treatment will facilitate the development of a technology for the controlled creation of a specific porous surface relief.

## 2. EXPERIMENTAL METHOD

Samples of a single crystal of silicon of a parallelepiped shape with dimensions  $1 \times 5 \times 0.35$  mm are used in the work. Gold film contacts are applied on the lateral faces of  $1 \times 5$  mm. One of the faces  $5 \times 0.35$  mm is irradiated by protons with the energy of 1.5 MeV and the energy dispersion below 150 eV (Fig. 1). The samples are irradiated using the high precision technique irradiation of the Kyiv scanning ion microprobe [9]. The proton beam is perpendicular to the face  $5 \times 0.35$  mm. The integral radiation fluence is  $2 \cdot 10^{14}$  p/cm<sup>2</sup>. In this case, accordingly to

the SRIM prediction [10], a layer about  $1.5\text{ }\mu\text{m}$  thick with a high density of radiation defects is expected to be obtained at the depth of  $30\text{ }\mu\text{m}$  beneath the irradiated surface.

This layer is created after irradiation, as it is evidenced by observations on an electron microscope 'HITACHI S-806'. For observations on an electron microscope the face  $1\times0.35\text{ mm}$  is processed. It is grinded by diamond films ( $1\text{ }\mu\text{m}$  diamond grain finish film) and is etched in a selective developer (HF with  $\text{HNO}_3$  and 1:40 ratio). Figure 2 shows the SEM image of the surface of this face. It is clearly seen that after irradiation with protons, a layer with characteristics different from those of the non-irradiated material is formed starting from the irradiated

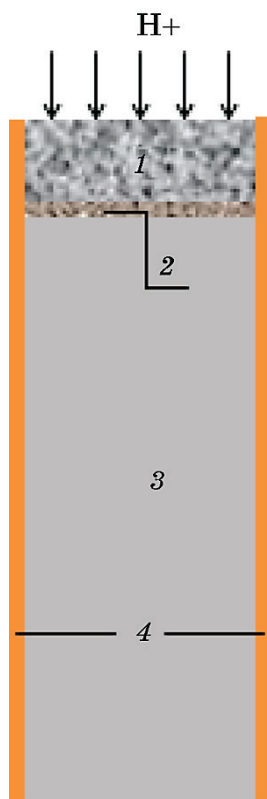


**Fig. 1.** The cross-section (dimensions  $1\times0.35\text{ mm}$ ) of the sample. The direction of irradiation with protons is specified by arrows. Designations: 1—cross-section of the surface layer after irradiation, part of the sample is exposed to irradiation where the number of defects increased; 2—cross-section of thin microlayer at the end of the movement of protons, saturated with hydrogen; 3—cross-section of the sample not exposed to radiation; 4—cross-section of the gold film contacts on the faces of  $1\times5\text{ mm}$ .

surface into the depth of the sample. The thickness of this layer is close to 30 microns.

At the edge of the irradiation is clearly visible a thin layer that actively interacted with the developer, which is associated with a large number of radiation defects. It should also be noted that the surface of the grinder in the layer that has been exposed to proton irradiation is finer-grained than the surface of the irradiated silicon. It is also noticeable that the grain size of the grinding surface gradually increases in the direction of the irradiated sample surface. In a layer about 9 microns thick from the surface, the irradiated grains are close to that at the depth of the sample. This clearly demonstrates that with irradiation, the number of radiation defects gradually increases in the direction of proton motion, and at the end of proton motion the number of radiation defects is very large.

Hydrogen treatment of materials in the condensed state can be done in various ways. We chose the cheapest and most efficient way, namely electrolytic saturation. The silicon wafer with gold contacts is mounted on the conductor substrate so that the contacts are connected to the substrate and the irradiated surface is on top. The conductive substrate and all faces of the sample except the irradiated face are securely isolated from contact with the electrolyte. Next, the sample is placed in a bath for electrolysis (Fig. 3). The upper irradiated surface perfectly contacted with the electrolyte. The conductive substrate and the gold contacts are connected to the negative pole of the current source for electrolysis. The positive pole of the current source is connected to a graphite electrode. Thus, during electrolysis, the upper irradiated surface of the sample served as a cathode and the graphite electrode is an anode. The tub is filled with a solution of 10%  $H_2SO_4$  and 2% KF in water.

A video camera is installed above the tub and during the electrolysis video control and video recording of the whole process took place.



**Fig. 2.** SEM images of face 1×0.35mm in electrons of secondary emission after irradiation by protons with energy of 1.5 MeV. The surface is sanded and chemically revealed.

Thus, the hydrogen treatment is given to the upper irradiated surface of the sample. During the flow of current from the irradiated surface, hydrogen is introduced into the sample. Electrolytic saturation with hydrogen occurred at room temperature. The current of electrolysis is 1 mA. During the electrolysis, small hydrogen bubbles are constantly formed on the surface. The density of hydrogen bubbles on the surface is visually identical and did not change during the electrolysis. That is, the entire surface of the sample worked uniformly throughout the electrolysis process.

The electrolysis process lasted for 10 minutes. After that time, the sample is destroyed. The gold contacts are naked to the electrolyte. Electric current has increased significantly. The electrolysis process is stopped. Subsequently, the substrate with the sample is removed from the bath. It is washed in distilled water and it is dried in running air at room temperature. The sample is then dismantled from the substrate. To do this, the varnish that isolated the conductors and the side surface of the sample is washed in acetone. The sample is detached from the substrate.

Observations in the optical microscope revealed that during the electrolysis a split of part of the sample is occurred. The two parts of the irradiated layer along the gold contacts are split on both sides along the entire sample. The side surfaces of the sample containing the remnants of gold contacts are also observed on an electron microscope.

Figure 4 provides the SEM image of a fragment of the side surface of the sample near the gold contact where the cleavage is occurred. It can be seen that the cleavage of part of the surface of the sample took place along a thin layer in the sample with a high concentration of defects

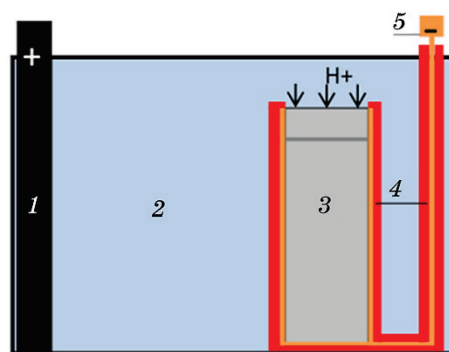


**Fig. 3.** The scheme of electrolytic hydrogen saturation of the sample. Designations: 1—graphite electrode (anode); 2—electrolyte (solution of 10%  $\text{H}_2\text{SO}_4$  and 2% KF in water); 3—the irradiated sample; 4—isolation of the sample and conductors from the electrolyte; 5—electrical connection of gold contacts to the negative pole of the current source (cathode).

after irradiation.

### 3. RESULTS AND DISCUSSION

Let's take a closer look at the processes that take place in Smart-Cut technology. During irradiation the movement of protons in the material results in a loss of energy. When the energy of the protons exceeds several keV, the energy losing is primarily due to the excitation of the electrons of the material and almost no collisions with the atoms of the substance are occurred. When the energy of the protons decreases, collisions with the atoms of the material occur, leading to the formation of radiation defects. If the movement of protons in the beam is not parallel, the formation of defects occurs at different depths from the surface. This leads to an increase in the thickness of the layer with radiation defects. The thickness of this layer is also affected by the iso-energy of the proton beam. The smaller the proton energy spread in the beam, the thinner the porous layer can form. At the end of the proton movement, the implantation of the material takes place. The implantation of hydrogen and the high density of radiation defects in the material creates a porous layer in which the pores are filled with hydrogen is obtained. Further separation of part of the crystal occurs during annealing due to the increase in temperature and pressure of hydrogen in the pores. Therefore, the primary purpose of proton irradiation in Smart Cut technology is to form a submicron layer with a high density of hydrogen-filled radiation defects. The implementation of Smart Cut technology requires a continuous beam of protons with a high proton

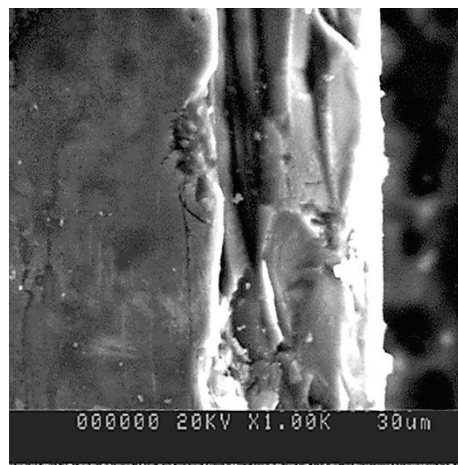


**Fig. 4.** The SEM image of the sample near the region of destruction, *i.e.* small region of the lateral surface near irradiated zone after cleavage of gold contact.

density and a small spread of proton energies in the beam.

Consider sequentially the physical processes in the sample during the processing provided in the paper. When the surface of the sample is exposed by protons with the energy of 1.5 MeV a thin layer in a large density of radiation defects occurs at a depth of about 30 microns from the surface. The thickness of this layer is 1.5–2.0  $\mu\text{m}$ . This is evidenced by both preliminary SRIM calculations [10] and electron microscope observations (Fig. 2). The integral radiation fluence is small and amounted to  $2 \cdot 10^{14} \text{ p/cm}^2$ . This is usually not a significant fluence of hydrogen implantation. Such a fluence is not enough to break away the surface. You should not even expect a split after annealing. Not enough cavities and hydrogen in this layer. Subsequent electrolysis contributed to the saturation of the hydrogen surface and the layer closest to it. Since the concentration of hydrogen is much lower in the surface, the hydrogen atoms diffused from the sample surface in the direction of the thin layer with radiation defects.

Based on the experimental data, the current density during electrolysis is  $57.15 \text{ mA/cm}^2$ . At such current density, estimate  $3.57 \cdot 10^{17} \text{ p/(s}\cdot\text{cm}^2)$  number of protons are supplied to the silicon surface every second. Usually, most of the hydrogen formed molecules and is bubbled into the air. A small fraction of this amount of hydrogen diffused into the sample. On the path of hydrogen diffusion, there is a thin layer with many radiation defects. Crystalline lattice defects are known to be good traps of hydrogen. These traps are capable of saturating high pressure hydrogen [11]. If at least one percent of the hydrogen coming to the sample surface during the electrolysis is trapped by radiation traps. This meant that the equivalent integral radiation fluence is  $2 \cdot 10^{20} \text{ p/cm}^2$ . Usually, during the electrolytic saturation of the sample with hydrogen, the saturation with hydrogen of the cavities formed during irradiation with protons occurred. The hydrogen pressure in these cavities increased and exceeded the tensile strength of silicon. These cavities have grown, they could unite. When enough is found in the sample of cavities with ‘beyond strength’ conditions, a split occurred.

What is the reason for the failure of the entire irradiated layer. In our view, this is primarily due to the poor layout of the gold contacts on the sample. Since the contacts are located on the sides, there is a potential distribution on the surface, in which the electrolytic current density is higher near the contacts and less on the middle of the surface. Because of this, a layer close to the gold contacts had advantages in hydrogen saturation. If the contact is placed on the surface opposite the irradiated one, the surface of the irradiated electric potential will be almost constant on the irradiated surface and the conditions for hydrogen saturation will be the same through the surface. That is, in such a case, uniform saturation of hydrogen is hypothetically possible

along the entire irradiated surface, and it is possible to expect a split during electrolysis of the entire irradiated layer. Secondly, the orientation of the surface of the single-crystal irradiated sample is chosen randomly and it did not create the conditions for the best cleavage of the layer. Of course, for a successful split of the surface layer, both considerations should be taken into account.

Let's talk separately about the prospects of using hydrogen treatment of semiconductor sample irradiated with protons to create a porous semiconductor surface. The less energy of the protons in the beam irradiated the surface of the semiconductor, the closer to the surface the layer with a high concentration of radiation defects will be. For example, for silicon, the energy of the protons in the beam will not exceed 10 keV when using irradiation to create a nanoporous surface [10]. In addition, it is possible to remove the requirement with the mono-energy of the proton beam. Subsequent saturation with hydrogen of the radiation defects will destroy the surface of the semiconductor that is before treatment. Nanoporous landscape is formed on the surface. It is well known that the constructing of complicated surface structures on the semiconductor by the electrochemical method is due to masks [12, 13]. The controllability of the proton beam enables the creation of an appropriate surface structure of the semiconductor without the use of masks.

#### 4. CONCLUSION

The analysis of the results obtained in this paper suggests that the electrolytic hydrogen saturation of a single crystal of silicon through a previously irradiated with protons surface with a small integral radiation fluence splits the irradiated surface of the sample. The irradiated surface splits along the layer with the highest concentration of radiation defects.

#### REFERENCES

1. V. A. Goltsov, A. G. Vasiljev, N. N. Vlasenko, and D. Fruchart, *Int. J. Hydrogen Energy*, **27**, Iss. 7–8: 765 (2002).
2. A. G. Vasiljev, N. N. Vlasenko, V. A. Goltsov, and D. Fruchart, *Metallofiz. Noveishie Tekhnol.*, **21**, No. 11: 87 (1999) (in Russian).
3. A. G. Vasiljev, *Metallofiz. Noveishie Tekhnol.*, **33**, No. 10: 1425 (2011) (in Russian).
4. A. G. Vasiljev, O. I. Kozonushchenko, T. A. Vasyliev, V. V. Zhuravel, and T. P. Doroshenko, *J. Nano- and Electronic Physics*, **11**, No. 3: 03003 (2019).
5. V. V. Kozlovskii, V. A. Kozlov, and V. N. Lomasov, *Semiconductors*, **34**: 123 (2000).
6. H. Föll, J. Carstensen, and S. Frey, *Journal of Nanomaterials*, **2006**, No. 1:

- 91635 (2006).
- 7. S. Doğan, N. Akın, C. Başköse, T. Asar, T. Memmedli, and S. Özçelik, *J. Mater. Sci. Eng. B*, **3**, No. 8: 518 (2013).
  - 8. W. Li, Z. Liu, F. Fontana, Y. Ding, D. Liu, J. T. Hirvonen, and H. A. Santos, *Adv. Mater.*, **30**, 24: 1703740 (2018).
  - 9. S. A. Lebed, O. G. Kukharenko, N. G. Tolmachov, and O. V. Tretiak, *Voprosy Atomnoy Nauki i Tekhniki*, No. 5(81): 131 (2012) (in Ukrainian).
  - 10. J. F. Ziegler, J. P. Biersack, and U. Liiemark, *Treatise on Heavy-Ion Science*, **1**: 93 (Boston: Springer: 1985).
  - 11. G. Alefeld and J. Völkl, *Hydrogen in Metals II. Series Topics in Applied Physics* (Berlin: Springer-Verlag: 1978).
  - 12. J. H. Park, Q. Wang, K. Zhu, A. J. Frank, and J. Y. Kim, *ACS Publications*, **4**, No. 22: 19772 (2019).
  - 13. S. H. Lee, J. S. Kang, and D. Kim, *Materials*, **11**, No. 12: 2557 (2018).